polarization effects. Scattering factors for neutral atoms and anomalous dispersion corrections for Ni, Br, and P were taken from ref 24. The structure was solved by Patterson and Fourier methods. An empirical absorption correction[25] was applied at the end of the isotropic refinement. Final refinement with fixed isotropic factors and coordinates for H atoms gave $R_F = 0.065$ and $R(w)_F = 0.070$. Most of the calculations were carried out with the X-Ray 80 system.[26]

Acknowledgment. We gratefully acknowledge generous support from the Dirección General de Investigación Científica y Técnica (Proyecto PB-87201), Junta de Andalucía, and the EEC (Grant SC1.0227.C). J. C. thanks the Spanish Ministry of Education (MEC) for a research grant. Thanks are also due to the University of Sevilla for the use of its analytical and NMR facilities.

Registry No. 1, 141612-15-9; 2, 141612-16-0; 3, 137515-87-8; 4, 141612-17-1; 5, 141612-18-2; 6, 141612-19-3; 7, 141612-20-6; 8, 137515-89-0; 9, 141612-21-7; 10, 141612-22-8; Ni(cod)$_2$, 1295-35-8; BrCH$_2$C$_6$H$_4$-*o*-Br, 3433-80-5.

Supplementary Material Available: Tables of H atom coordinates and thermal parameters for 6 (2 pages). Ordering information is given on any current masthead page.

OM910705X

---

[24] *International Tables for X-Ray Crystallography*; Kynoch Press: Birmingham, U.K., 1974; Vol. IV, p 72.

[25] Walker, N.; Stuart, D. *Acta Crystallogr.* **1983**, *A39*, 158.

[26] Stewart, J. M. *The X-Ray 80 System*; Computer Science Center, University of Maryland: College Park, MD, 1985.

Mechanism for the Exchange Processes Observed in the Compounds $[M(\eta\text{-}C_5H_5)_2(\eta\text{-}RCH{=}CH_2)H]$ (M = Nb, Ta)

Malcolm L. H. Green,* Andrea Sella,† and Luet-Lok Wong

Inorganic Chemistry Laboratory, South Parks Road, Oxford OX1 3QR, U.K.

Received September 11, 1991

The fluxional processes in the compounds *exo*-$[M(\eta\text{-}C_5H_5)_2(\eta\text{-}CH_3CH{=}CH_2)H]$ (M = Nb, Ta) have been investigated by magnetization and spin-saturation transfer and two-dimensional exchange NMR techniques. Rate constants for three separate processes have been determined. A mechanism involving agostic η^2-alkyl ligands is proposed.

Bercaw and co-workers recently reported a NMR study of the dynamic processes in the olefin–hydride complexes $[M(\eta\text{-}C_5R''_5)_2(\eta\text{-}RCH{=}CH_2)H]$ (M = Nb, Ta) and proposed a multistep mechanism to account for the data.[1] We have made studies of the similar dynamic behavior of other olefin–hydride–metal systems, and these have provided evidence for the occurrence of intermediates with agostic bonds and in-place rotation of agostic metal–alkyl groups.[2] We were interested to see if agostic intermediates can also account for the dynamic processes oberved for the niobium and tantalum systems. We deemed such a study to be worthwhile since the insertion of olefins into the metal–hydride bonds in olefin–hydride complexes and its microscopic reverse, β-elimination, are reactions of fundamental importance in organometallic chemistry and are key steps in such industrial catalytic processes as hydroformylation, olefin hydrogenation, and isomerization.[3,4]

A preliminary account of this work has been reported.[5]

Background

The mechanism generally proposed for the reversible insertion of an olefin into a metal–hydride bond[3,4] proceeds via a planar, delocalized cyclic transition state in which the migrating hydrogen is bonded to both the metal center and to one of the olefinic carbons, thus resulting in overall cis addition of the metal–hydride to the double bond:[6]

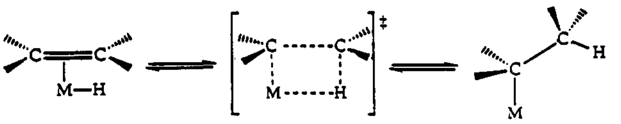

Strong supporting evidence for this delocalized transition state (or intermediate) comes from the discovery of transition-metal–alkyl complexes with β-agostic interactions in which this delocalized structure is adopted in the ground state.[7] Indeed, many complexes which were previously assigned ethylene–hydride structures have since been shown to be agostic ethyl complexes with 2e–3c M←H–C$_\beta$ interactions.

Since olefin insertions are often reversible and not rate-limiting, direct measurements of their kinetics in reaction sequences are difficult. Notably, however, Halpern and co-workers have been successful in measuring the rate of olefin insertion into rhodium–hydride bonds in the reaction of various olefins with a number of rhodium complexes.[8,9] Reversible intramolecular olefin insertion resulting in mutual exchanges has been observed by variable-temperature NMR spectra and/or by deuterium labeling, and in some cases the rate constants and activation

---

* To whom correspondence should be addressed.

† Department of Chemistry, University College London, 20 Gordon Street, London WC1H 0AJ, U.K.

[1] Burger, B. J.; Santarsiero, B. D.; Trimmer, M. S.; Bercaw, J. E. *J. Am. Chem. Soc.* **1988**, *110*, 3134–3146.

[2] Green, M. L. H.; Wong, L.-L. *J. Chem. Soc., Chem. Commun.* **1988**, 677–679. Green, M. L. H.; Wong, L.-L. *New J. Chem.* **1989**, *10*, 747–752.

[3] Parshall, G. A. *Homogeneous Catalysis*; Wiley: New York, 1980.

[4] Collman, J. P.; Hegedus, L. S.; Norton, J. R.; Finke, R. G. *Principles and Applications of Organotransition Metal Chemistry*, 2nd ed.; University Science Books: Mill Valley, CA, 1987.

[5] Bercaw, J. E.; Burger, B. J.; Green M. L. H.; Santarsiero, B. D.; Sella, A.; Trimmer, M.; Wong, L.-L. *J. Chem. Soc., Chem. Commun.* **1989**, 734–736.

[6] Labinger, J. A.; Hart, D. W.; Seibert, W. E., III; Schwartz, J. *J. Am. Chem. Soc.* **1975**, *97*, 3851–3852. Nakamura, A.; Otsuka, S. *J. Am. Chem. Soc.* **1973**, *95*, 7262–7272.

[7] Brookhart, M.; Green, M. L. H. *J. Organomet. Chem.* **1983**, *250*, 395–408. Brookhart, M.; Green, M. L. H.; Wong, L.-L. *Prog. Inorg. Chem.* **1988**, *36* 1–124.

[8] Halpern, J.; Okamoto, T.; Zakhariev, A. *J. Mol. Catal.* **1976**, *2*, 65–68.

[9] Halpern, J.; Okamoto, T. *Inorg. Chim. Acta* **1984**, *89*, L53–L54.

0276-7333/92/2311-2650$03.00/0 © 1992 American Chemical Society

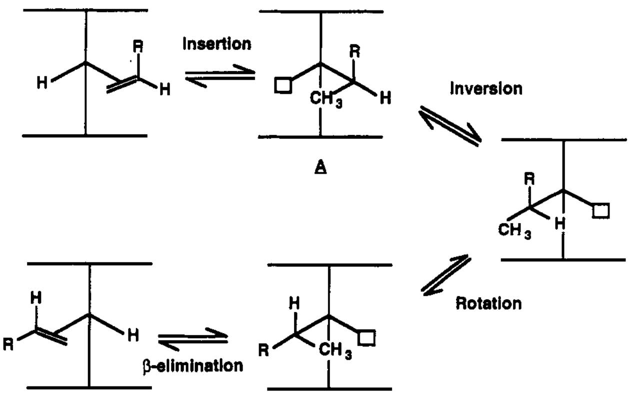

Figure 1. Mechanism proposed by Bercaw (Ia), showing the inversion step. In this figure we adopt a modified form of the Newman diagram, the two C_5 rings being represented by the two hirozontal lines.

parameters have been measured by NMR magnetization transfer techniques.[10]

Appreciation of the Results and Mechanisms Presented by Bercaw

The complexes [$M(\eta\text{-}C_5R''_5)_2(\eta\text{-}RCH{=}CH_2)H$] ($R''$ = H, M = Nb (1), Ta (2);[1] R'' = Me, M = Nb (3), Ta (4);[11] R''_5 = Me_4Ph, M = Ta[12]) can exist as exo and endo isomers. For the $\eta\text{-}C_5H_5$ compounds 1 and 2, both the exo and endo isomers are found, whereas for the $\eta\text{-}C_5Me_5$ analogues 3 and 4, only the endo isomers are observed. Exo ↔ endo isomerization in 1 and 2, which occurs by olefin rotation, is slow on the chemical time scale even at elevated temperatures, and distinct isomers are observed in the NMR spectra. The low symmetry of both isomers (C_1) results in the two C_5 rings and the vinylic hydrogens of the olefin being both chemically and spectroscopically inequivalent.

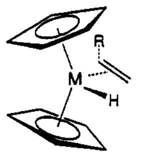

exo-1

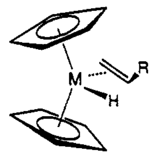

endo-1

The olefin–hydride complexes 1–4 are fluxional. The endo isomers undergo exchange of the hydride with the methine hydrogen, and this process also causes the two C_5 rings to become equivalent at the same rate.[1,11] For the exo isomers, however, it was found that exchange between the hydride and the methylene hydrogens was much faster (1–2 orders of magnitude) than the exchange between the C_5 rings. For the exo propene–hydride compound 1 (R = Me) there is an additional exchange process whereby the Nb–H exchanges not only with both of the methylene hydrogens but also with the hydrogens of the exo methyl group. The initial analysis of this four-site exchange system was simplified by treating the two inequivalent methylene hydrogens and the hydride as one site, thus reducing the exchange process to a two-site problem.[1] The analysis gave similar rates of exchange of the Nb–H and the methylene hydrogens, k_1, and the exo methyl group, k_2. Both of these rate constants were considerably greater than that for the exchange between the inequivalent C_5 rings, k_3. Thus, for the endo isomers $k_1 = k_3$ and for the exo isomers, for R = aryl, $k_1 \gg k_3$ and, for R = Me, $k_1 \approx k_2 \gg k_3$.

The mechanism Ia given in Figure 1 was put forward to account for the exchange processes of the exo isomers.[1] As shown, the olefin inserts into the metal–hydride bond, forming a 16-electron σ-alkyl species (A) in which the metal center has a "pyramidal" structure. Rotation of the methyl group about the C_α–C_β bond followed by β-elimination leads to exchange between the hydride and the methylene hydrogens. In order to effect exchange between the C_5 rings, it is necessary for the σ-alkyl group to rotate about the M–C_α bond and for the metal center to invert so as to bring the methyl group to the correct orientation for the β-elimination step. The slower rate of the C_5 ring exchange process was proposed to arise from a non-negligible barrier to either the rotation about the M–C_α bond or to the inversion of the metal center.

A key proposal of mechanism Ia is the pyramidal geometry of the metal center in the 16-electron σ-alkyl intermediate A formed by olefin insertion. In their seminal paper on bent metallocenes, Lauher and Hoffmann considered the structure of such alkyl complexes.[13] Their extended Hückel calculations indicate that for d^1, d^3, and low-spin d^2 systems the pyramidal structure would be slightly stabilized relative to the trigonal structure:

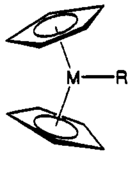

Trigonal

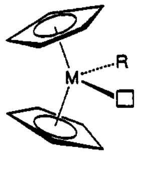

Pyramidal

However, high-spin d^2 systems were predicted to be symmetrical at the metal center. In support of this, both of the two high-spin d^2 metallocene compounds whose crystal structures have been reported, namely [$V(\eta\text{-}C_5H_5)_2Cl$][14] and {[$Ti(\eta\text{-}C_5Me_5)_2]_2(\mu\text{-}N_2)$},[15] have been shown to have trigonal structures. Further, the compound [$Ti(\eta\text{-}C_5Me_5)_2Cl$] is trigonal, even though it has a d^1 configuration,[16] and the 16-electron high-spin pentadienyl cation [$Fe(\eta\text{-}C_5H_7)(PEt_3)_2$]$^+$ also possesses a plane of symmetry.[17]

Therefore, we feel that there are no compelling arguments for a pyramidal intermediate such as A or, even if the intermediate was pyramidal, no significant inversion barrier to inversion would be expected. Indeed, we question the proposals of inversion barriers in other 16-electron intermediates.[18-20]

---

[10] (a) Werner, H.; Feser, R. *J. Organomet. Chem.* **1982**, *232*, 351–370. (b) Werner, R.; Werner, H. *J. Organomet. Chem.* **1979**, *174*, C63–C66. Werner, R.; Werner, H. *Chem. Ber.* **1983**, *116*, 2074–2087. Werner, H.; Kletzin, R.; Hohn, A.; Paul, W.; Knaup, W.; Ziegler, M. L.; Serhadli, O. *J. Organomet. Chem.* **1982**, *306*, 227–239. (c) Roe, D. C. *J. Am. Chem. Soc.* **1983**, *105*, 7771–7772. (d) Roe, D. C. Personal communication. (e) Bunting, H. E.; Green, M. L. H.; Newman, P. A. *J. Chem. Soc., Dalton Trans.* **1988**, 557–577. (f) Brookhart, M.; Green, M. L. H.; Pardy, R. B. A. *J. Chem. Soc., Chem. Commun.* **1983**, 691–693. (g) Byrne, J. W.; Kress, J. R. M.; Osborn, J.; Ricard, L.; Weiss, R. E. *J. Chem. Soc., Chem. Commun.* **1977**, 662–663. (h) Chaudret, B. N.; Cole-Hamilton, D. J.; Wilkinson, G. *Acta Chem. Scand., Ser. A* **1978**, *A32*, 763–769. (i) Cracknell, R. B.; Orpen, A. G.; Spencer, J. L. *J. Chem. Soc., Chem. Commun.* **1984**, 326–328. Cracknell, R. B.; Orpen, A. G.; Spencer, J. L. *J. Chem. Soc., Chem. Commun.* **1986**, 1005–1006.

[11] Doherty, N. M.; Bercaw, J. E. *J. Am. Chem. Soc.* **1985**, *107*, 2670–2681.

[12] Parkin, G.; Bunel, E.; Burger, B. J.; Trimmer, M. S.; Van Asselt, A.; Bercaw, J. E. *J. Mol. Catal.* **1987**, *41*, 21–39.

[13] Lauher, J. W.; Hoffmann, R. *J. Am. Chem. Soc.* **1976**, *98*, 1729–1742.

[14] Fieselmann, B. F.; Stucky G. D. *J. Organomet. Chem.* **1977**, *137*, 43–54.

[15] The magnetic moment of this complex is significantly less than the "spin-only" value, an observation which remains unexplained: Sanner, R. D.; Duggan, D. M.; McKenzie, T. C.; Marsh, R. E.; Bercaw, J. E. *J. Am. Chem. Soc.* **1976**, *98*, 8358–8365.

[16] Pattiasina, J. W.; Heeres, H. J.; van Bolhuis, F.; Meetsma, A.; Teuben, J.; Spek, A. L. *Organometallics* **1987**, *6*, 1004–1010.

[17] Bleeke, J. R. Personal communication.

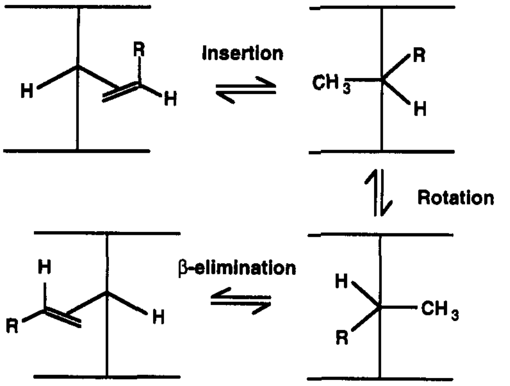

Figure 2. Modified Bercaw mechanism (Ib) with an effectively 16-electron trigonal intermediate.

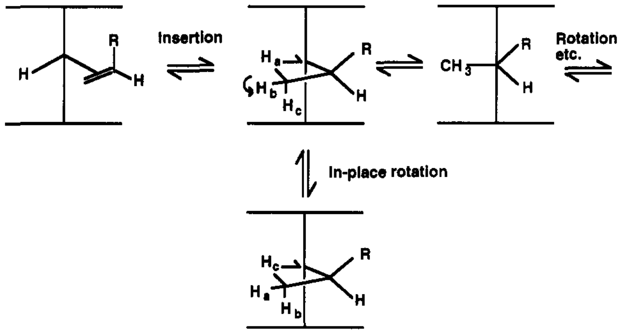

Figure 3. New mechanism (II) proceeding via in-place rotation in 18-electron agostic alkyl intermediates.

If the coordinatively unsaturated intermediate A is effectively symmetrical, then a modified version of mechanism Ia, namely mechanism Ib, may be considered and this is shown in Figure 2. In mechanism Ib the difference in the exchange rate constants can only arise as a result of restricted (slow) rotation of the alkyl group about the M–C_α bond (vide infra).

Proposed New Mechanism and Comparative Comments

We now consider a different mechanism which invokes 18-electron β-agostic alkyl intermediates in which the agostic bonds cause what amounts to an electronic restriction to alkyl rotation in the dynamic processes. This new mechanism, II, is shown in Figure 3 and incorporates an in-place rotation of a β-agostic alkyl intermediate. An in-place (nondissociative) rotation mechanism for hydrogen scrambling in a ground-state agostic alkyl group was first proposed by Cotton and Stanislowski to account for the dynamic processes in [Mo{$Et_2B(pz)_2$}$(CO)_2$(η-CH_2CHRCH_2)] (R = H, Ph; pz = pyrazolyl).[21] Similar metal–alkyl intermediates, and in particular an in-place rotation step, have been proposed for hydrogen scrambling in the olefin–hydride complexes {[Mo(dppen)$_2$(η-C_2H_4)$_2$H][CF_3CO_2]} (dppen = *cis*-$Ph_2PCH{=}CHPPh_2$),[2] [W(η-C_5H_5)$_2$(*exo*-$CH_3CH{=}CH_2$)H]$^+$,[22] and [Re(η-C_5H_5)(CO)$_2$(η-C_2H_3R)H]$^+$.[23] Spencer and co-workers considered the possibility of an in-place rotation mechanism in their recent study of {Pt[(*t*-Bu)$_2$PCH$_2$CH$_2$P(*t*-Bu)$_2$](η^2-Et)}$^+$ (η^2-Et refers to a β-agostic ethyl group).[20] We note, however, that in their study of hydrogen scrambling in the agostic cobalt system [Co(η-C_5H_5)(PR_3)(η^2-Et)]$^+$ Orpen and Spencer marginally disfavored a mechanism involving an in-place rotation on the grounds that an extended Hückel calculation suggested it to be energetically unfavorable relative to dissociation.[10i]

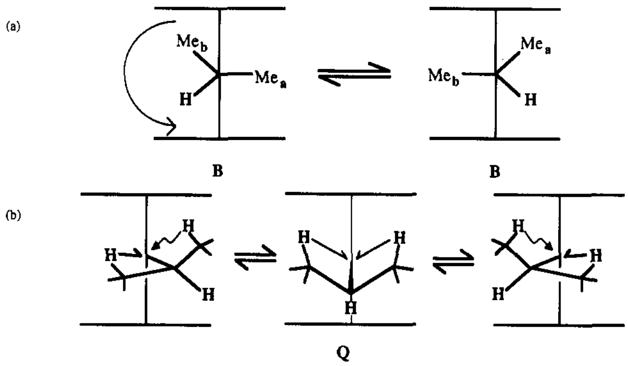

Figure 4. (a) The 60° isopropyl rock. (b) Intermediate Q.

In mechanism II exchange between the methylene hydrogens and the hydride occurs via in-place rotation about the C_α–C_β bond of the agostic alkyl intermediate. For the endo isomers this process is necessarily accompanied by exchange of the C_5 rings, i.e. $k_1 = k_3$, as is observed. For the exo isomers, on the other hand, exchange of the C_5 rings occurs via the rate-limiting dissociation of the agostic hydrogen from the metal center in the η^2-alkyl intermediate to form a 16-electron σ-alkyl intermediate, in which the alkyl group undergoes rapid rotation about the M–C_α bond. Hence in mechanism II, the higher barriers to C_5 ring scrambling arise from the extra energy necessary to break the agostic interaction in the η^2-alkyl intermediate.

We now consider how the alternative mechanisms Ib and II can account for the scrambling processes in the exo propene compounds 1 and 2 (R = Me), whereby the hydride undergoes exchange with the methyl hydrogens. It will be seen that the important difference between the two mechanisms is the nature of the barrier to rotation of the σ-alkyl group in the intermediates and whether the origin of this barrier is steric (mechanism Ib) or electronic via agostic interactions (mechanism II).

In mechanism Ib, propene insertion gives the 16-electron σ-isopropyl intermediates B, which must have the asymmetric rotational group-state structure shown in Figure 4a. A 120° rotation in an anticlockwise direction of the σ-isopropyl group about the M–C_α bond in B followed by β-elimination will result in exchange of the C_5 rings. However, rotation by only 60° in the clockwise direction (isopropyl rock) followed by β-elimination results in exchange of the hydride with the exo methyl group *without* scrambling of the C_5 rings.

In mechanism II, the agostic η^3-isopropyl transition state Q is proposed to account for the exchange of the hydride with the hydrogens of the exo methyl group while the inequivalence of the C_5 rings is maintained. This step is shown in Figure 4b and involves the displacement of the existing agostic bond by a new one formed by a C–H bond of the exo methyl group. This reaction could be facilitated by coupling the attack of the exo methyl group with the vibrational mode in the intermediate which brings the α-carbon atom toward the plane containing the ring centroids and the metal center.

At the transition state Q both C–H bonds involved in the displacement reaction are coordinated to the metal center. Thus, a simple 16-electron σ-isopropyl complex

---

(18) Elian, M.; Hoffmann, R. *Inorg. Chem.* **1975**, *14* 1058–1076. Hofmann, P. *Angew. Chem., Int. Ed. Engl.* **1977**, *8*, 536–537 and references therein.

(19) Brookhart, M.; Buck, R. C.; Danielson, E. *J. Am. Chem. Soc.* **1989**, *111*, 567–574.

(20) Mole, L.; Spencer, J. L.; Carr, N.; Orpen, A. G. *Organometallics* **1991**, *12*, 49–52.

(21) Cotton, F. A.; Stanislowski, A. G. *J. Am. Chem. Soc.* **1974**, *96*, 5074–5082.

(22) McNally, J. P.; Copper, N. J. *Organometallics* **1988**, *7*, 1704–1715.

(23) Casey, C. P.; Yi, C. S. *Organometallics* **1991**, *10*, 33–35.

is not formed during this formally associative substitution reaction. The processes shown in Figure 4 are very similar. In both cases the isopropyl group must rotate by approximately 60° before β-elimination. Exchange of the C_5 rings in mechanism II occurs, as for other R = aryl compounds, by the higher energy process of breaking the agostic bond. If the barriers to the isopropyl rock or the formation of Q are larger than those of the β-elimination steps, then $k_1 > k_2$. If on the other hand these barriers, then $k_1 = k_2$. It was therefore important to attempt to determine these two rate constants accurately, without any simplifying assumptions. This was the main objective of the experiments described below.

Determination of the Kinetics of the Dynamic Processes

The compounds 1 and 2, where R = Me, were prepared by the reaction of $[M(\eta\text{-}C_5H_5)_2Cl_2]$ with an excess of isopropylmagnesium bromide:

$$[M(\eta\text{-}C_5H_5)_2Cl_2] \xrightarrow[Et_2O]{i\text{-PrMgBr}} [M(\eta\text{-}C_5H_5)_2(CH_3CH{=}CH_2)H]$$

$$M = Nb, Ta$$

The isopropyl reagent is preferable to the *n*-propyl analogue, as the latter gives nonequilibrium ratios of the endo and exo isomers and samples must then be thermally equilibrated before kinetic measurements can be made. The ^1H NMR spectra of the compounds showed them to be >95% pure.

The extreme sensitivity of the compounds to oxygen and moisture made the synthesis and sample preparation tedious, and the thermal instability of the complexes precluded the use of NMR line-shape analysis techniques. Three different dynamic NMR techniques were used in the kinetic measurements. Thus, the rate constants of the four-site exchange system consisting of the exo methyl group, the inequivalent methylene hydrogens, and the hydride ligand in the tantalum exo propene–hydride complex 2 (R = Me) were determined using multisite NMR spin saturation transfer,[24-26] ^{13}C NMR magnetization transfer (a stack plot of a typical experiment is shown in Figure 5), and quantitative phase-sensitive ^1H–^1H two-dimensional exchange (PSEXSY) NMR experiments (a typical spectrum is shown in Figure 6).[27] The exchange system in the niobium analogue 1 (R = Me) was analyzed by multisite NMR spin saturation transfer techniques because significant decomposition occurred during the relatively long times required for an PSEXSY experiment. It was, however, possible to perform a small number of ^{13}C NMR magnetization transfer experiments for the niobium compound. These experiments proved to be especially difficult and were therefore only carried out at a single temperature. The measured magnetization transfer rate constants are reported in Table I.

Our system is a non-equally-populated four-site exchange in which two mechanisms, responsible for k_1 and k_2, respectively, may be thought to be operating concurrently. The procedure used to calculate the correct chemical rate constants for a problem in which parallel exchange processes occur is outlined in the Appendix and will be discussed fully elsewhere.[28] The correct chemical rate data are shown in Table II. The data show that for R = Me and M = Nb $k_1 \approx 2k_2 \gg k_3$ and for R = Me and M = Ta $k_1 \approx k_2 \gg k_3$.[29]

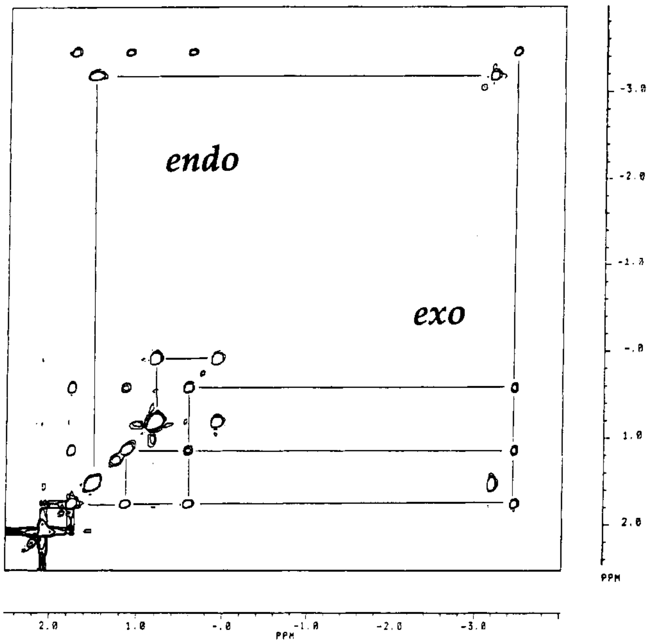

Figure 5. Two-dimensional ^1H–^1H PSEXSY NMR spectrum for $[Ta(\eta\text{-}C_5H_5)_2(\eta\text{-}CH_2{=}CHCH_3)H]$ acquired at 360 K. The exchange network in the exo isomer is shown below, and that for the endo isomer above, the diagonal peaks.

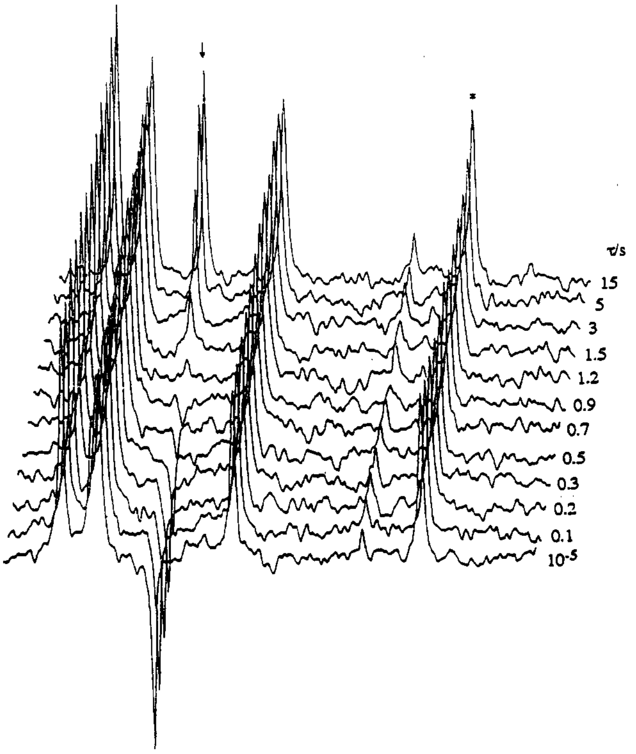

Figure 6. ^{13}C magnetization transfer experiment for $[Ta(\eta\text{-}C_5H_5)_2(\eta\text{-}CH_2{=}CHCH_3)H]$ at 357 K. The arrow denotes the inverted CH_2 resonance, and the asterisk indicates the methyl resonance.

---

[24] Sandström, J. *Dynamic NMR Spectroscopy*; Academic Press: London, 1982; Chapter 4.

[25] Hoffmann, R. A.; Forsén, S. *Prog. NMR Spectrosc.* **1966**, *1*, 15–204 (particularly 89–94).

[26] Ugurbil, K. *J. Magn. Reson.* **1985**, *64*, 207–219.

[27] Meier, B. H.; Ernst, R. R. *J. Am. Chem. Soc.* **1979**, *101*, 6441–6442. Jeener, J.; Meier, B. H.; Bachmann, P.; Ernst, R. R. *J. Phys. Chem.* **1979**, *71*, 4546–4553.

[28] Green, M. L. H.; Sella, A.; Wong, L.-L. *Organometallics*, following paper in this issue.

[29] Our failure to observe magnetization transfer between the two C_5 resonances in the ^1H and ^{13}C NMR spectra of 1 and 2, respectively, at the highest temperatures studied, is inconsistent with the coalescence data reported in ref 1. Owing to sample decomposition, Trimmer measured the coalescence temperatures under an atmosphere of propene. The possibility of an associative exchange of propene cannot therefore be excluded.

Table I. Magnetization Transfer Rate Constants[a] for Hydrogen Scrambling in [*exo*-M(η-C_5H_5)$_2$(η-$CH_3CH{=}CH_2$)H] (M = Nb, Ta)

M = Nb			M = Ta							
T/K	$k(CH_3 \rightarrow H)^b$	$k(H \rightarrow CH)^b$	*T*/K	$k(CH_3 \rightarrow H)^b$	$k(H \rightarrow CH)^b$	*T*/K	$k(CH_3 \rightarrow H)^c$	$k(H \rightarrow CH)^c$	*T*/K	$k(CH_3 \rightarrow CH_2)^d$
293	0.03 (1)	0.13 (2)	337	0.035 (3)	0.038 (6)	350	0.08 (1)	0.109 (2)	347	0.24 (7)
298[e]	0.06 (1)	0.27 (2)	347	0.08 (3)	0.09 (1)	360	0.29 (2)	0.34 (2)	357	0.60 (7)
303	0.09 (1)	0.49 (4)	357	0.24 (3)	0.26 (4)	365	0.37 (2)	0.46 (2)		
313	0.33 (4)	1.34 (13)								

[a] Reported in s^{-1}; standard deviations ($n \approx 6$) are in parentheses. [b] Multisite NMR spin saturation transfer (SST) data only. [c] 2-D EXSY data. [d] Carbon-13 NMR magnetization transfer data. [e] $k_{MT}(CH_2 \rightarrow CH_3)$ = 0.20 (5) on the basis of ^{13}C magnetization transfer experiments.

Table II. Chemical Rate Constants[a] for Hydrogen Scrambling in [*exo*-M(η-C_5H_5)$_2$(η-$CH_3CH{=}CH_2$)H] (M = Nb, Ta)

M = Nb			M = Ta						
T/K	$k_2{}^b$	$k_1{}^b$	*T*/K	$k_2{}^b$	*T*/K	$k_2{}^c$	$k_1{}^c$	*T*/K	$k_2{}^d$
293	0.18 (6)	0.30 (6)	337	0.22 (3)	350	0.48 (6)	0.65 (12)	347	0.48 (9)
298[e]	0.36 (6)	0.63 (6)	347	0.50 (12)	360	1.74 (12)	2.04 (12)	357	1.20 (10)
303	0.54 (6)	1.20 (12)	357	1.49 (20)	365	2.22 (12)	2.76 (12)		
313	1.98 (24)	3.03 (39)							

[a] Reported in s^{-1}; standard deviations ($n \approx 6$) are in parentheses. For the relation of chemical to magnetization transfer rate constants, see the Appendix. [b] Based on multisite NMR spin saturation transfer (SST) data only. [c] Based on two-dimensional PSEXSY data. [d] Carbon-13 NMR magnetization transfer data. [e] k_2 = 0.40 (7) on the basis of ^{13}C NMR magnetization transfer experiments.

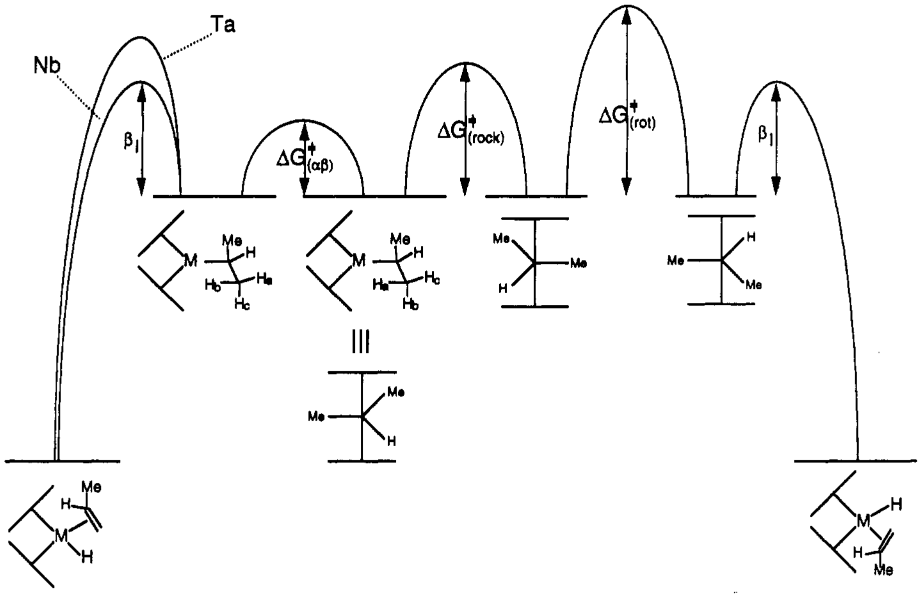

Figure 7. Schematic energy profile for mechanism Ib.

These new kinetic data can be discussed with reference to the respective qualitative free energy diagrams for mechanisms Ib and II. A number of important differences between these mechanisms are thereby revealed. An approximate free energy diagram of the exchange processes in the niobium complex 1 (R = Me) via mechanism Ib is shown in Figure 7. The 16-electron σ-isopropyl intermediate formed by propene insertion is stabilized relative to the transition state by β_I, the barrier to β-elimination. Rotation about the C_α–C_β bond (with a barrier $\Delta G^\ddagger(\alpha\beta)$ which should be at least the value in propane—ca. 17 kJ mol^{-1}), which leads to scrambling of the hydride with the methylene hydrogens of the propene, is generally *assumed* to be much faster than olefin insertion, and $\Delta G^\ddagger(\alpha\beta) \ll \beta_I$. This assumption is commonly invoked and allows the properly weighted exchange rate constant to be equated with some elementary step, such as olefin insertion,[11] and the differences between the activation barriers to be discussed in terms of substituent effects etc. The observation that $k_3 < 0.04$ s^{-1} at 313 K (see Experimental Section) implies that the barrier to the 120° rotation, $\Delta G^\ddagger$(rot), is higher than $\Delta G^\ddagger$(rock) and hence β_I by >10 kJ mol^{-1}. In other words, the barrier to the 60° isopropyl rock is smaller than that for the 120° rotation, but they are both higher than β_I, the barrier to β-elimination. For the tantalum compound 2 (R = Me), $\Delta G^\ddagger(\text{rock}) < \beta_I$, and therefore $k_2 = k_1$. The observation that $k_3 < 0.04$ s^{-1} at 363 K corresponds to $\Delta G^\ddagger(\text{rot}) - \beta_I > 10$ kJ mol^{-1}.

A schematic free energy diagram for mechanism II is shown in Figure 8. Olefin insertion gives an 18-electron agostic alkyl intermediate with an associated barrier to β-elimination of β_{II}. As the NMR spectra have not given evidence for the intermediates, this suggests their concentration is probably less than 0.1%. This implies that any intermediates lie at least 20 kJ mol^{-1} above the ground state. The data do not indicate the relative sizes of the barriers to in-place rotation ($\Delta G^\ddagger$(ipr)) and β-elimination (β_{II}), but we assume that the former is the larger (vide infra). For the niobium complex 1 (R = Me), therefore, the barrier to the transition state Q, $\Delta G^\ddagger$(Q), is higher than $\Delta G^\ddagger$(ipr). The smaller value of k_3 suggests that the barrier to the formation of the 16-electron σ-isopropyl intermediate by dissociation of the agostic hydrogen from the metal center, $\Delta G^\ddagger$(diss), is higher than $\Delta G^\ddagger$(Q) and hence $\Delta G^\ddagger$(ipr) by >10 kJ mol^{-1}. For the tantalum complex 2 (R = Me), both $\Delta G^\ddagger$(ipr) and $\Delta G^\ddagger$(Q) are lower than β_{II},

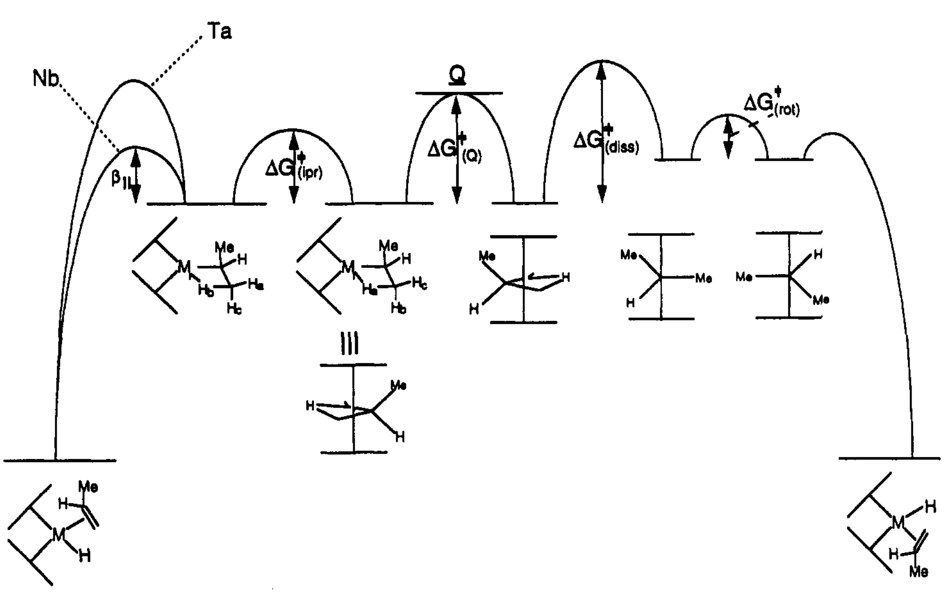

Figure 8. Schematic energy profile for mechanism II.

and so $k_2 = k_1$. The lower value of k_3 implies that ΔG^* (diss) is higher than β_{II} by >10 kJ mol^{-1}. Hence, *both* mechanisms can account for the experimental observations and the kinetic data in Table II alone do not distinguish between them.

Consideration of the Mechanisms in the Light of Circumstantial Evidence

The proposed transition state Q in the exo methyl to M–H exchange process via mechanism II is at first sight unusual but is in fact not unique. We note that there are many examples of related agostic-alkyl ↔ alkyl interchanges in organometallic enyl complexes of the type $[\overline{\text{Mn}(\eta\text{-C}_6\text{H}_8\text{-H}})(\text{CO})_3]$[7]

$$\overline{\text{C–H M—H–C}} \leftrightarrow \overline{\text{C–H—M H–C}}$$

Furthermore, the η^3-isopropyl system in the transition state Q, with two agostic hydrogens, is clearly similar to that in the transition state of the in-place rotation step. Such "doubly agostic" species have also been proposed to occur in the "coordinated alkane" intermediates or transition states of the mechanism of intramolecular hydrogen scrambling observed in the alkyl hydride complexes $[Rh(\eta\text{-}C_5Me_5)(PMe_3)(n\text{-}C_3H_5)H]$,[30] $[W(\eta\text{-}C_5R_5)_2(Me)H]$ (R = H,[31] Me[32]), and $[Re(\eta\text{-}C_5H_5)_2(Me)H]^+$.[33] Organo-transition-metal and organoactinide complexes with more than one agostic M—H–C bond in the ground state have been structurally characterized. For example, the two α-C–H groups of one of the benzyl ligands in $[Ti(\eta\text{-}C_5Me_5)(CH_2Ph)_3]$,[34] and those of one of the neopentyl ligands in $[Th(\eta\text{-}C_5Me_5)_2(CH_2CMe_3)_2]$,[35] have been shown to participate in agostic interactions with the metal centers. Similarly, the α- and one of the γ-hydrogens of the bis(trimethylsilyl)methyl group in $[Y(\eta\text{-}C_5Me_5)_2\{CH(SiMe_3)_2\}]$ form agostic bonds with the yttrium center.[36] In this system Teuben and co-workers have attributed a barrier to restricted rotation about the C–Si bond to the γ-agostic interaction. In mechanism II we therefore have an electronic origin for a rotational barrier in a metal–alkyl group, namely agostic bonding.

In the case of mechanism Ib, for which no electronic factors are invoked, restrictions to the isopropyl rock and 120° rotation must arise from interligand contacts. The observed rate constant trends can be readily rationalized: the barriers to the rotation processes of an isopropyl group are expected to increase in the following order: about the C_α–C_β bond < isopropyl rock < full rotation about the M–C_α bond. It is important to note, however, that in order to observe differential rate constants the last two barriers must be higher than that of β-elimination.

We therefore turned to the literature for quantitative estimates of rotational barriers about the metal–carbon bond in metal alkyl and aryl complexes. There have been few systematic studies on such barriers in organo-transition-metal compounds, and there are no examples of such work on $M(\eta\text{-}C_5R_5)_2R$ complexes of direct relevance.[37] Of the reported studies, the rotation barriers for compounds with small alkyl groups (Me, Et, *n*-Pr) are often too low to be measured by traditional NMR techniques.[38,39] A number of recent studies are of interest in the present context. Rotation of the isopropyl group in $[W(\eta\text{-}C_5H_5)_2(CHMe_2)Cl]$ could not be monitored by NMR methods,[22] but a barrier of 35.5 kJ mol^{-1} was obtained for isopropyl rotation in $[U(\eta\text{-}C_5H_5)_3(i\text{-}Pr)]$.[40] Our attempts to measure the M–C_{ipso} bond rotation barrier in $[Nb(\eta\text{-}C_5H_5)_2(C_6H_5)(CO)]$ were inconclusive: both the ^1H and ^{13}C NMR spectra were invariant in the temperature range 203–298 K. Brookhart and co-workers have observed the collapse of the 16-electron intermediate $[Fe(\eta\text{-}C_5H_5)$-

---

(30) Periana, R. A.; Bergman, R. G. *J. Am. Chem. Soc.* **1986**, *108*, 7332–7346.

(31) Bullock, R. M.; Headford, C. E. L.; Hennessy, K. M.; Kegley, S. E.; Norton, J. R. *J. Am. Chem. Soc.* **1989**, *111*, 3897–3908.

(32) Parkin, G.; Bercaw, J. E. *Organometallics* **1989**, *8*, 1172–1179.

(33) Gould, G. I.; Heinekey, D. M. *J. Am. Chem. Soc.* **1989**, *111*, 5502–5504.

(34) Mena, M.; Pellinghelli, M. A.; Royo, P.; Serrano, R.; Tiripicchio, A. *J. Chem. Soc., Chem. Commun.* **1986**, 1118–1119.

(35) Bruno, J. W.; Smith, G. M.; Marks, T. J.; Fair, C. K.; Schultz, A. J.; Williams, J. L. *J. Am. Chem. Soc.* **1986**, *108*, 40–56.

(36) den Haan, K. H.; de Boer, L. J.; Teuben, J. H.; Spek, A. L.; Kojic-Prodic, B.; Hays, G. H.; Huis, R. *Organometallics* **1986**, *5*, 1726–1733.

(37) Mann, B. E. In *Comprehensive Organometallic Chemistry*; Abel, E. W., Stone, F. G. A., Wilkinson, G., Eds.; Pergamon Press: Oxford, U.K., 1982; Vol. 3, Chapter 20, p 99.

(38) Stanley, K.; Baird, M. C. *J. Am. Chem. Soc.* **1975**, *97*, 4292–4298 and references therein.

(39) Jordan, R. F.; Norton, J. R. *J. Am. Chem. Soc.* **1979**, *101*, 4853–4858. Jordan, R. F.; Tsang, E.; Norton, J. R. *J. Organomet. Chem.* **1978**, *149*, C53–C56.

(40) Marks, T. J.; Seyam, A.; Kolb, J. R. *J. Am. Chem. Soc.* **1972**, *95*, 5529–5539.

(CO)CH_2Ph], generated by laser flash photolysis, from which an upper limit of 27.2 kJ mol^{-1} can be inferred for the barrier to the rotation of the benzyl group.[19]

In compounds with bulky ancillary ligands (e.g. η-C_5Me_5) and/or bulky alkyl groups (e.g mesityl, bis(trimethylsilyl)methyl) the rotation barriers are sufficiently high for the process to be studied by dynamic NMR methods.[41] It appears that, in most cases, the reported data have not been corrected by the appropriate population weighting factors.[42] However, this correction has only a small effect on the activation barriers. The relevant examples for bent metallocene systems show that the trends of rotation barriers are not always straightforward. Thus, although increasing the bulk of the C_5 ring increases the barrier to tolyl rotation in $[M(\eta\text{-}C_5Me_4H)(\eta\text{-}C_5R_5)(p\text{-tolyl})_2]$ (M = Ti, Zr; R_5 = H_5, Me_4H, Me_5[41i]), the rotation barriers in $\{Zr(\eta\text{-}C_5H_5)_2[CH(SiMe_3)_2]R\}$ *decrease* with an increase in the steric demand of the R group.[41a] Also, for the compounds $[Ti(\eta\text{-}C_5Me_4H)_2(p\text{-tolyl})X]$, the rotation barriers for X = Cl, Br, I were greater than that for X = *p*-tolyl.[41a,b] Finally, coalescence temperatures in the closely related $\{Zr(\eta\text{-}C_5H_4R)_2[CH(SiMe_3)_2]Cl\}$ (R = H, Me, Et, *i*-Pr, *t*-Bu, $SiMe_3$) suggest barriers in the range 59.3–65.2 kJ mol^{-1}.[41c]

For the isopropyl-rock step in mechanism Ib, the α-hydrogen has to move across the plane containing the ring centroids and the metal center such that at the transition state this hydrogen is pointing directly toward one of the C_5 rings (see Figure 2) and there is no eclipsing of the methyl groups and the C_5 rings. The barrier to this step can be expected to be low. Thus, we have examined the rotation of the isopropyl group in the intermediate A using the molecular graphics program CHEMX.[43] The coordinates used for defining the molecule were taken from the X-ray crystal structure of $[Nb(\eta\text{-}C_5H_5)_2(\eta\text{-}CH_2{=}CH_2)(CH_2CH_3)]$.[44] An isopropyl group was constructed from the ethyl ligand using standard bond lengths and angles, and the Nb–C_α vector was aligned with the C_2 axis of the metallocene fragment. Assuming that the Nb–C_α distance is unchanged in the intermediate (2.53 Å), this gives a closest contact between the methyl and cyclopentadienyl hydrogens of approximately 1.6 Å when the alkyl group is rotated about the M–C_α axis (Figure 9). Although this appears at first sight to indicate a substantial interaction between the ligands in the transition state (the van der Waals radius of hydrogen is 1.17 Å), an energy minimization calculation suggests a barrier <24 kJ mol^{-1}. This value must be treated with caution since the potentials have not been "calibrated" using related known systems, but it is a further indication that the barrier to the rotation about the M–C_α bond can be expected to be quite low.

It may therefore be concluded that it is only with alkyl groups much larger than isopropyls that barriers to rotation are readily measurable (to be observable by common methods, $\Delta G^\ddagger$ must in general be greater than ca. 35 kJ mol^{-1}). Thus, it is reasonable to expect that $\Delta G^\ddagger$(rot) and, in particular, $\Delta G^\ddagger$(rock) in mechanism Ib for **1** and **2** (R = Me) should be small (<35 kJ mol^{-1}). If this is taken with the *assumption* that $\beta_I \gg \Delta G^\ddagger(\alpha\beta)$, it is likely that both $\Delta G^\ddagger$(rot) and $\Delta G^\ddagger$(rock) are less than β_I. Hence, we suggest that mechanism Ib is not unambiguously established on the basis of the observed data.

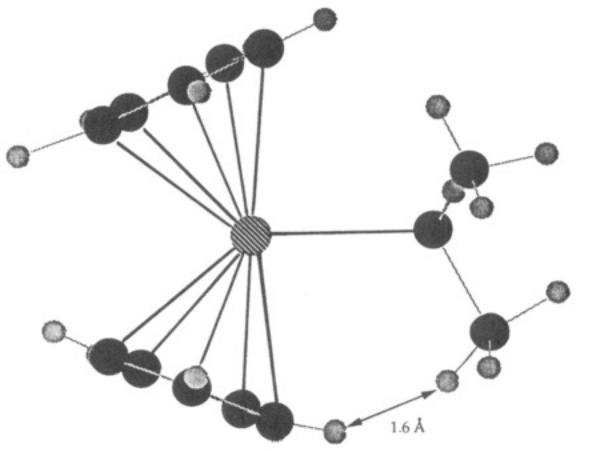

Figure 9. CHEMX view of the proposed 16-electron $[Nb(\eta\text{-}C_5H_5)_2(CHMe_2)]$ intermediate.

Alternatively, one may argue that the 16-electron alkyl intermediate lies close in energy to the transition state to β-elimination. In other words, the barrier to rotation about the C_α–C_β bond is of the same order of magnitude as that to β-elimination; $\Delta G^\ddagger(\alpha\beta) \geq \beta_I$. It is then possible for mechanism Ib to account for the observed data. However, this *new assumption* implies that the significance of rotational barriers has been underestimated and that the barriers in other olefin–hydride exchange processes can no longer be attributed solely to the insertion step itself but, rather, must include significant yet unquantifiable contributions from restricted rotations about C–C and M–C bonds. If this is indeed the case, then the direct correlation of the observed barriers with stereoelectronic effects at the metal becomes less straightforward.

We have shown that $k_1 \approx 2k_2$ for **1** (R = Me) while $k_1 \approx k_2$ for **2** (R = Me). In mechanism II this arises from the different strengths of the agostic bonds to second- and third-row elements, although no direct thermochemical study of relative agostic bond strengths has yet been reported.[45] Hence, the barrier to β-elimination (β_{II}) and that to the formation of the 16-electron σ-alkyl ($\Delta G^\ddagger$(diss)) are higher in the tantalum complex **2** (R = Me). Thus, mechanism II can readily account for our observations. In addition, the slower rates of exchange for the tantalum complexes may be accounted for in terms of the ground-state stabilization which arises from the stronger M–H bond strengths for the third-row metals over those for the second row.[46]

There are other examples in the literature where the question also arises of whether slow rotation of an alkyl group involved in dynamic processes results from steric or agostic interactions. Thus, the dynamic NMR studies on the complexes $[M(\eta\text{-}CH_2CHCH_2)_3R]$ (M = Mo, W; R = Et, *n*-Pr, *i*-Pr), reported recently by Jolly and co-

---

[41] (a) Sharp, P. R.; Astruc, D.; Schrock, R. R. *J. Organomet. Chem.* **1979**, *182*, 477–488. (b) Jones, W. D.; Feher, F. J. *Inorg. Chem.* **1984**, *23*, 2376–2388. (c) Jeffery, J.; Lappert, M. F.; Luong-Thi, N. T.; Atwood, J. L.; Hunter, W. E. *J. Am. Chem. Soc., Chem. Commun.* **1978**, 1081–1083. Jeffrey, J.; Lappert, M. F.; Luong-Thi, N. Y.; Webb, M.; Atwood, J. L. *J. Chem. Soc., Dalton Trans.* **1981**, 1593–1605. (d) Courtot, P.; Labed, V.; Pichon, R.; Salaün, J. Y. *J. Organomet. Chem.* **1989**, *359*, C9–C11. (e) Salaün, J. Y. Personal communication. (f) Lappert, M. F.; Riley, P. I.; Yarrow, P. I. W.; Atwood, J. L.; Hunter, W. E.; Zaworotko, M. J. *J. Chem. Soc., Dalton Trans.* **1982**, 814–827. (g) Green, M. L. H.; Lindsell, W. E. *J. Chem. Soc. A* **1969**, 2215–2118. (h) Nakamura, A.; Otsuka, S. *J. Am. Chem. Soc.* **1972**, *94*, 1886–1894. (i) Schock, L. E.; Brock, C. P.; Marks, T. J. *Organometallics* **1987**, *6*, 232–241.

[42] Johnson, C. S.; Moreland, C. G. *J. Chem. Educ.* **1973**, *70*, 477–483. We note that, in an article on rotational barriers, no explicit mention of these corrections is made (Kessler, H. *Angew. Chem., Int. Ed. Engl.* **1970**, *9*, 219–225) and such questions remain controversial (Faller, J. *Adv. Organomet. Chem.* **1977**, *16*, 211–239).

[43] CHEMX, Chemical Design Ltd., Oxford, U.K.

[44] Guggenberger, L. J.; Meakin, P.; Tebbe, F. N. *J. Am. Chem. Soc.* **1974**, *96*, 5420–5427.

[45] We note that studies of dissociation energies of η^2-alkane from $M(CO)_5$ (M = Cr, Mo, W) fragments have failed to show significant differences between Mo and W; see: Kang, G. K.; Vaida, V.; Peters, K. S. *Polyhedron* **1988**, *7*, 1619–1622 and references therein.

[46] Cox, D. N.; Roulet, R. *J. Chem. Soc., Chem. Commun.* **1989**, 175–176.

workers,[47] are relevant. The compounds were shown to have β-agostic alkyl groups. For the isopropyl compounds, it was found that while the agostic hydrogen underwent rapid exchange with the other hydrogens of the agostic β-methyl group even below 173 K, there was no observable exchange between the agostic methyl and uncoordinated methyl groups. Casey and Yi reported hydrogen scrambling exclusively between the hydride and the proximal olefin hydrogens in the complexes $[Re(\eta\text{-}C_5H_5)(CO)_2(\eta\text{-}C_2H_3R)H]^+$ and proposed a mechanism involving in-place rotation in agostic alkyl intermediates which are not free to rotate about the Re–C_α bond.[23] Mulvey and co-workers have recently observed restricted rotation of the phenyl groups of {[PhC(H)NC(H)Ph]Na(PMDETA)} (PMDETA) = $(Me_2NCH_2CH_2)_2NMe$), a complex shown by X-ray crystallography to have an agostic ground-state structure.[48] Similarly restricted rotation in α-agostic benzyl complexes of titanium has been noted by Serrano and co-workers.[49]

Conclusions

We have shown that for the compounds **1** and **2** we can account for the observation that the stereochemistry of the metal centers, i.e. the inequivalence of the C_5 rings, is maintained while there is observable exchange between the hydride and the methylene hydrogens by invoking some mechanism for restricted rotation of the alkyl groups in the intermediates. We disfavor mechanism Ia on the grounds that there is no evidence for significant inversion barriers in the 16-electron bent metallocene alkyl intermediates. We note, however, that there is no *direct* evidence to distinguish between steric restriction (mechanism Ib) and electronic (agostic) restriction (mechanism II). We disfavor mechanism Ib because the available data on sterically-induced barriers to rotation of the small σ-alkyl group about the M–C_α bond, which control the rate constants, suggest them to be too low to account for the data. Further quantitative data on such rotation barriers are needed to clarify this issue. In mechanism II the alkyl groups in the intermediates are "tied down" by the metal center via agostic interactions. Once these interactions are broken, the alkyl groups are free to rotate and scramble the two C_5 rings. Thus, we believe the proposal of agostic interactions (an electronic restriction) to be a more compelling explanation than that of interligand steric interactions.

Having seen how agostic interactions can have a direct influence on stereochemistry in olefin–hydride systems, one might speculate on the possibility that agostic intermediates may also participate in chemical processes. The possible role of α-agostic interactions in maintaining the stereochemistry of metal centers and thus determining the stereochemical outcome of reactions has been stressed by Cooper in the dissociative exchange of CH_3CN in the tungsten complex $[W(\eta^5\text{-}C_5H_4OR^*)(\eta\text{-}C_5H_5)(NCCH_3)Me]^+$ (R^* = CHPh(*i*-Pr))[50] and by Bercaw in the stereospecific polymerization of propene catalyzed by the scandium complex $[Sc\{(\eta\text{-}C_5Me_4)_2SiMe_2\}(H)]$.[51] Agostic alkyl intermediates may also be involved in the classic carbonyl migratory insertion reaction. In particular, the remarkable configurational stability of the unsaturated acyl complexes which are proposed to be the intermediates might perhaps be due to agostic interactions. Although calculations by Hoffmann and others[18] suggest that the metal center should be configurationally stable in some of the classic model systems, Carmona has recently reported the η^2-agostic acyl complex $[Mo(Me_2NCS_2)(PMe_3)_2(CO)(\eta^2\text{-}COCH_2H)]$.[52] We note that a number of closely related compounds are fluxional, undergoing reversible insertion at room temperature.[53] It may be possible to test these ideas by examining deuterium isotope effects in these systems. Experiments to this end are in progress.[54] In addition, solid-state NMR studies aimed at obtaining direct evidence for in-place rotation are currently in progress.

Experimental Details

All preparations, manipulations, and reactions were carried out under an inert atmosphere of dinitrogen (<5 ppm of oxygen, <20 ppm of water) using standard Schlenk tube and vacuum line techniques and using flame-dried glassware predried in an oven or in a drybox. Solutions were filtered through filter sticks equipped with glass microfiber filter disks predried at >150 °C overnight. Dinitrogen was purified by passage through a column containing BASF catalyst and 5-Å molecular sieves.

Solvents were predried over activated 5-Å molecular sieves and then distilled from sodium–potassium alloy (petroleum ether (bp 40–60 °C), diethyl ether, pentane) under an inert atmosphere of dinitrogen before use. All solvents were thoroughly deoxygenated by repeated evacuation followed by readmission of dinitrogen. All solvents, including $[^2H_6]$benzene and $[^2H_8]$toluene for NMR samples, were stored over sodium–potassium alloy in glass ampules equipped with a Teflon stopcock (Young's). Solvents for NMR spectroscopy were transferred using pipets in the drybox. The solutions were then filtered through a plug of glass wool directly into an NMR tube equipped with a PTFE stopcock which had been stored in an oven at >150 °C overnight and cooled under vacuum. A freshly prepared sample was used for each dynamic NMR experiment.

The propene–hydride complexes $[M(\eta\text{-}C_5H_5)_2(\eta\text{-}CH_3CH{=}CH_2)H]$ (M = Nb,[55] Ta[56]) were prepared as described. The extreme sensitivity of these compounds cannot be overemphasized (we note that Teuben was unable to report analytical data for the niobium compounds), and exceptional care is required in their preparation and handling. The presence of water/oxygen is signaled for the niobium compound by the appearance of a blue/green color probably attributable to the formation of blue μ-oxo dimers.[57] Thermal decomposition appears to be autocatalytic; thus, the initial purity of the sample is crucial.

$[Nb(\eta\text{-}C_5H_5)_2(C_6H_5)(CO)]$ was prepared by the method of Bercaw.[58]

^1H and ^{13}C NMR spectra were determined at 300 and 75.4 MHz, respectively, using a Bruker AM-300 spectrometer with standard 5- and 10-mm broad-band probes, respectively. Spectra were calibrated internally using the residual solvent (^1H) or solvent (^{13}C) resonances and are reported relative to tetramethylsilane (δ 0 ppm). Two-dimensional NMR experiments were acquired using standard Bruker software and processed using the ASPECT 3000 computer. Probe temperatures in variable-temperature NMR experiments were measured with an independently cali-

---

(47) Benn, R.; Holle, S.; Jolly, P. W.; Mynott, R.; Romão, C. C. *Angew. Chem., Int. Ed. Engl.* **1986**, *25*, 555–557. Benn, R.; Brock, T. H.; Jolly, P. W.; Rufinska, A.; Schroth, G. *Polyhedron* **1990**, *9*, 23–34.

(48) Andrews, P. C.; Mulvey, R. E.; Clegg, W.; Reed, D. *J. Organomet. Chem.* **1990**, *386*, 287–297.

(49) Gomez-Sal, M. P.; Mena, M.; Royo, P.; Serrano, R. *J. Organomet. Chem.* **1988**, *358*, 147–159 and references therein.

(50) McNally, J. P.; Cooper, N. J. *J. Am. Chem. Soc.* **1989**, *111*, 4500–4502.

(51) Piers, W.; Bercaw, J. E. *J. Am. Chem. Soc.* **1990**, *112*, 9406–9407.

(52) Carmona, E.; Sanchez, L.; Marin, J. M.; Poveda, M. L.; Atwood, J. L.; Priester, R. D.; Rodgers, R. D. *J. Am. Chem. Soc.* **1984**, *106*, 3214–3222.

(53) Carmona, E.; Contreras, L.; Poveda, M. L.; Sanchez, L. J. *J. Am. Chem. Soc.* **1991**, *113*, 4322–4324.

(54) Carmona, E. Personal communication.

(55) Klazinga, A. H.; Teuben, J. H. *J. Organomet. Chem.* **1980**, *194*, 309–316.

(56) Klazinga, A. H.; Teuben, J. H. *J. Organomet. Chem.* **1978**, *157*, 413–419.

(57) Kirillova, N. I.; Lemenovskii, D. A.; Baukova, T. V.; Struchkov, Yu. T. *Koord. Khim.* **1977**, *3*, 1600. Green, M. L. H.; Hughes, A. K.; Mountford, P. *J. Chem. Soc., Dalton Trans.* **1991**, 1407–1416.

(58) Threlkel, R. S.; Bercaw, J. E. *J. Am. Chem. Soc.* **1981**, *103*, 2650–2659.

brated thermocouple immersed in the appropriate volume of toluene in an NMR tube before and after the experiments. The values given in the Tables are accurate to within ±1.0 °C.

Phase-Sensitive ^{1}H-^{1}H 2D Exchange (PSEXSY) NMR Experiments on 2 (R = Me). The standard pulse sequence D1-π/2-D0-π/2-D9-π/2-FID for the phase-sensitive PSEXSY experiment using time proportional phase increment (TPPI) methods was used with a recycling time D1 = 1 s. The mixing time D9 was varied randomly by ±25% between scans by the computer to remove scalar *J*-coupling effects—the number of transients per increment was greater than 16 to ensure that this variation was sufficiently random. A typical experiment required 12 h. In each experiment 256 increments of 1K words each were recorded, giving a two-dimensional data matrix of 256K workds. The F1 dimension was zero-filled, but no zero-filling was applied in the F2 dimension, resulting in a transformed matrix of 1028K words. Rate constants from the volume integrals of a larger data matrix of 4096K words obtained by zero-filling in both the F1 and F2 dimensions were not significantly different. The diagonal peaks were phased to have negative intensities. Thus, transient nuclear Overhauser effects would be expected to give cross peaks of positive intensities while chemical exchange would give cross-peaks having negative intensities. A PSEXY spectrum at a temperature where exchange is slow shows cross peaks of positive intensities which were barely detectable (<0.5% of the intensities of the diagonal peaks), suggesting that transient NOE's can be ignored. Depending on their magnitude and sign, scalar couplings give rise to cross peaks of both positive and negative intensities in the two-dimensional NMR spectrum. Such cross peaks, which can be expected to have unusual line shapes, were absent from the spectrum, suggesting that the effects of scalar coupling are either minimal or have been removed by the random variations in D9.

The values of the magnetization transfer rate constants given in Table I are the mean and standard deviations obtained from at least seven experiments. The PSEXSY experiments were repeated at each temperature using different mixing times D9; typical values are 0.5, 1, and 2 s at each temperature. The FID's in the two-dimensional data files were premultiplied with shifted sine-bell-squared apodization functions (mild signal-to-noise enhancement) before the 2-D Fourier transform. Volume integrals of the diagonal and cross peaks were used as inputs for the D2DNMR program.[59,60]

Multisite ^{1}H NMR Spin Saturation Transfer Experiments. The method used was based on the experiments described by Hoffmann and Forsén.[24,25] Thus, if the four exchanging sites in the propene hydride complexes are labeled H (hydride), Me (the exo methyl group), and CH$_a$ and CH$_b$ (the vinylic hydrogens), eq 1 can be written for the hydride, where M_0(H) is the equilibrium

$$\frac{\mathrm{d}M_z(\mathrm{H})}{\mathrm{d}t} = \frac{M_0(\mathrm{H}) - M_z(\mathrm{H})}{T_1(\mathrm{H})} - M_z(\mathrm{H})[2k_{\mathrm{MT}}(\mathrm{H}\rightarrow\mathrm{CH}) + k_{\mathrm{MT}}(\mathrm{H}\rightarrow\mathrm{Me})] + M_z(\mathrm{Me})[k_{\mathrm{MT}}(\mathrm{Me}\rightarrow\mathrm{H})] + k_{\mathrm{MT}}(\mathrm{CH}\rightarrow\mathrm{H})[M_z(\mathrm{CH_a}) + M_z(\mathrm{CH_b})] \quad (1)$$

magnetization of the hydride, the M_z's are the magnetizations at time *t*, and the rate constants refer to the forward processes denoted by the direction of the arrow. For all mechanisms, $k_{\mathrm{MT}}(\mathrm{H}\rightarrow\mathrm{CH_a}) = k_{\mathrm{MT}}(\mathrm{H}\rightarrow\mathrm{CH_b})$ and $k_{\mathrm{MT}}(\mathrm{CH_a}\rightarrow\mathrm{H}) = k_{\mathrm{MT}}(\mathrm{CH_b}\rightarrow\mathrm{H})$.

If the resonances due to the methyl group and both the methylene hydrogens are saturated, then all the terms in M_z other than that due to the hydride in eq 1 reduce to zero and we have eq 2. At the equilibrium state for three-site saturation dM_z(H)/d*t* = 0, and we have eq 4. Thus, the ratio of the equilibrium

$$\frac{\mathrm{d}M_z(\mathrm{H})}{\mathrm{d}t} = \frac{M_0(\mathrm{H})}{T_1(\mathrm{H})} - \frac{M_z(\mathrm{H})}{\tau_1(\mathrm{H})} \quad (2)$$

$$1/\tau_1(\mathrm{H}) = 2k_{\mathrm{MT}}(\mathrm{H}\rightarrow\mathrm{CH}) + k_{\mathrm{MT}}(\mathrm{H}\rightarrow\mathrm{Me}) + 1/T_1(\mathrm{H}) \quad (3)$$

$$\frac{M_0(\mathrm{H})}{T_1(\mathrm{H})} = \frac{M_\infty(\mathrm{H, 3\ sites})}{\tau_1(\mathrm{H})} \Rightarrow \frac{M_\infty(\mathrm{H, 3\ sites})}{M_0(\mathrm{H})} = \frac{\tau_1(\mathrm{H})}{T_1(\mathrm{H})} \quad (4)$$

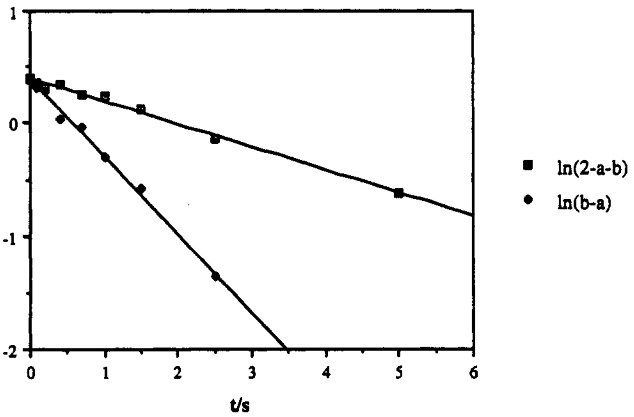

Figure 10. Typical plot of the ^{13}C magnetization transfer data recorded at 357 K. For details of the analysis, see the Experimental Section.

magnetizations of the hydride with and without irradiation of the three other sites gives the ratio of the values of τ_1(H) and T_1(H). Integration of eq 2 gives eq 5. *C* is a constant whose value depends

$$M_z(\mathrm{H}) = M_0(\mathrm{H})[C\exp(-t/\tau_1(\mathrm{H})) + M_\infty(\mathrm{H, 3\ sites})] \quad (5)$$

on the conditions at *t* = 0. From eq 5 a plot of ln [M_z(H) – M_∞(H, 3 sites)] vs time *t* gives a straight line with slope $-1/\tau_1$(H). The value of T_1(H) can be calculated from the ratio shown in eq 4 and the sum of the rate constants from eq 3.

To measure the individual forward rate constants, two of the four exchanging sites are saturated. Thus, if the resonances due to the methylene hydrogens are saturated, eq 1 reduces to eq 6.

$$\frac{\mathrm{d}M_z(\mathrm{H})}{\mathrm{d}t} = \frac{M_0(\mathrm{H})}{T_1(\mathrm{H})} - M_z(\mathrm{H})[1/T_1(\mathrm{H}) - 2k_{\mathrm{MT}}(\mathrm{H}\rightarrow\mathrm{CH}) + k_{\mathrm{MT}}(\mathrm{H}\rightarrow\mathrm{Me})] + M_z(\mathrm{Me})[k_{\mathrm{MT}}(\mathrm{Me}\rightarrow\mathrm{H})] \quad (6)$$

At equilibrium, dM_z(H)/d*t* = 0, and substituting eqs 3 and 4 into 6, we have eq 7. All the parameters in eq 7 except the rate

$$\frac{M_\infty(\mathrm{H, 3\ sites}) - M_\infty(\mathrm{H, 2\ sites})}{\tau_1(\mathrm{H})} + M_\infty(\mathrm{Me})[k_{\mathrm{MT}}(\mathrm{Me}\rightarrow\mathrm{H})] = 0 \quad (7)$$

constant can be experimentally determined; thus, it is possible to calculate k_{MT}(Me→H). Since by mass balance k_{MT}(H→Me) = 3k_{MT}(Me→H), the value of k_{MT}(H→CH) can be calculated using eq 3. Further, if the resonances due to the methyl group and one of the methylene hydrogens are saturated, it is possible to calculate k_{MT}(H→CH) from eq 3. This serves as a self-consistency check on the rate constants thus derived.

Multisite irradiations in the SST experiments were carried out by sequential low-power irradiation of the desired number of sites for 100–200 ms with a switching time of 5 ms between sites (decoupler gated off). The total irradiation time was varied by cycling through the frequency list by the necessary number of times. The assumption is that, during the switching and irradiation time of one site, there is insufficient time for the zeroed magnetization of the site(s) previously irradiated to recover significantly. Trial experiments showed that this assumption is reasonable: the relaxation of a saturated resonance during the switching and irradiation times was less than 5%. This arises from the relatively long T_1 values (>1.5 s) of the hydrogens concerned. The plots of ln [M_z(H) – M_∞(H, 3 sites)] vs *t* were analyzed by standard least-squares fitting procedures. Data from a typical experiment are shown in Figure 10. Values of 1/τ_1(H) obtained from different experiments at a given temperature agreed to within ±7%. Six or seven experiments were carried out at each temperature.

There was no saturation transfer between the two C$_5$ ring resonances of 1 (R = Me) at 313 K, thus allowing an upper limit of 1/9T_1 or ca. 0.02 s^{-1} to be estimated for k_{MT}(Cp→Cp).

---

(59) Abel, E. W.; Coston, T. P. J.; Orrell, K. G.; Šik, V.; Stephenson, D. *J. Magn. Reson.* **1986**, *70*, 34–53.

(60) Abel, E. W.; Moss, I.; Orrell, K. G.; Šik, V.; Stephenson, D. *J. Chem. Soc., Dalton Trans.* **1987**, 2695–2701.

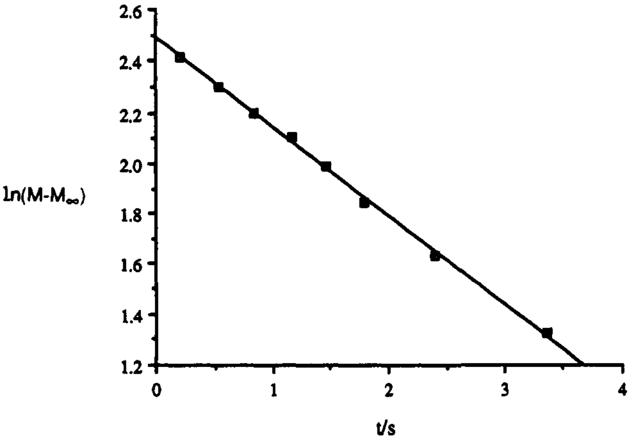

Figure 11. Plot of ln $(M - M_\infty)$ vs t for a typical data set from multisite spin saturation transfer experiments. For details of the analysis, see the experimental section.

^{13}C NMR Magnetization Transfer Experiments on 2 (R = Me). Magnetization transfer was examined by selective inversion. The selective π pulse was generated using the DANTE pulse sequence.[61] Typically a series of 40 4-μs pulses, each separated by a 1-ms delay, was used. Delays of between 1 μs and 30 s were used between the selective π and the $\pi/2$ read pulses. To minimize errors due principally to sample decomposition during an overnight run, the sets of measurements were obtained in blocks of four scans. The spectra were stored on disk, and each new block was added at the end of each set of delays. This was done so as to give a final total of about 80 scans per delay. A microprogram was written to implement this procedure. It was not possible to detect the exchange of the C_5 rings in 2 (R = Me) by this technique at 363 K. Measurements were precluded by extensive sample decomposition at 393 K. It is therefore possible to estimate an upper limit of $k_{MT}(Cp \rightarrow Cp)$ at 363 K as ca. $1/9T_1$, or 0.02 s^{-1}. For the exo methyl to methylene carbon exchange process, the normal simplifying assumption that the T_1 values of the two sites are equal applies.

Data analysis was carried out as follows.[62] For a two-site exchange in which we selectively invert one site, the magnetizations in the two sites at any given time, t, are denoted and a and b. These may be normalized by dividing by the magnetizations at infinite time. The magnetizations are governed by the modified Bloch equations:

$$\frac{da}{dt} = -\frac{1}{T_1}(a - a_\infty) - (a - b)k_{MT}$$

$$\frac{db}{dt} = -\frac{1}{T_1}(b - b_\infty) + (a - b)k_{MT}$$

At infinite time the normalized intensities are given by $a_\infty = b_\infty = 1$. Taking sums and differences, we have

$$\frac{d(a+b)}{dt} = \frac{1}{T_1}[2 - (a + b)]$$

$$\frac{d(b-a)}{dt} = -\left(\frac{1}{T_1} + 2k_{MT}\right)(b - a)$$

Thus, after integration a plot of ln $[2 - a - b]$ against magnetization transfer delay, t, gives a straight line with slope $-(1/T_1)$. Similarly, a plot of ln $[b - a]$ against t gives a straight line with gradient $-[(1/T_1) + 2k]$. A typical data set is plotted in Figure 11.

Acknowledgment. We wish to thank NATO (research grant 287-84) for support and the Gas Research Institute for partial support of this work. We thank Professor E. W. Abel, Dr. K. G. Orrell, and Dr. D. Stephenson for a copy of the D2DNMR program. We are grateful to Prof. J. E. Bercaw, Prof. M. S. Brookhart, Prof. E. Carmona-Guzman, Dr. C. M. Dobson, Prof. J. W. Faller, Dr. S. J. Heyes, Dr. B. E. Mann, Dr. D. O'Hare, Prof. G. Parkin, and Dr. M. S. Trimmer for enlightening discussions.

Appendix: Determination of the Rate Constants for the Exchange Processes

For an N-spin system, the Kubo–Sack matrix consists of an $N \times N$ array in which the off-diagonal elements are given by the rate constants for magnetization transfer from site i to site j:

$$D_{ij} = k_{ij}$$

and where the diagonal elements are given by

$$D_{ii} = -\sum_i k_{ij} \qquad i \neq j$$

In attempting to relate the measured rate constants to chemically meaningful rate constants, it is usually necessary to factor out a chemical (or exchange) rate constant, which corresponds to the rate constant for the chemical event, k_{chem}, be this a restricted rotation, an insertion, or simply a libration, which results in the observed magnetization transfer. When this has been done, the individual matrix elements simply represent the probability of spins in site i being transferred to site j.

In the case of a system in which concurrent rate processes operate, it is necessary to separate the overall K-S matrix into a series of submatrices, each of which refers to a separate exchange process.

Thus, in the propene hydride system, we may view the two rate processes as being composed of in-place rotation, k_1, and the isopropyl rock, k_2. Constructing the Kubo–Sack matrices for the two cases, we obtain

$$\begin{bmatrix} -^2/_3 & ^1/_3 & ^1/_3 & 0 \\ ^1/_3 & -^2/_3 & ^1/_3 & 0 \\ ^1/_3 & ^1/_3 & -^2/_3 & 0 \\ 0 & 0 & 0 & 0 \end{bmatrix} k_1 + \begin{bmatrix} -^5/_6 & ^1/_6 & ^1/_6 & ^3/_6 \\ ^1/_6 & -^5/_6 & ^1/_6 & ^3/_6 \\ ^1/_6 & ^1/_6 & -^5/_6 & ^3/_6 \\ ^1/_6 & ^1/_6 & ^1/_6 & -^3/_6 \end{bmatrix} k_2$$

Hence, the measured rate constant $k_{MT}(CH_3 \rightarrow H)$ is related to k_2 by

$$k_{MT}(CH_3 \rightarrow H) = {}^1/_6 k_2$$

Measurement of $k_{MT}(CH_3 \rightarrow H)$, is therefore, a direct measure of k_2.

On the other hand, $k_{MT}(H \rightarrow CH)$ is given by

$$k_{MT}(H \rightarrow CH) = {}^1/_3 k_1 + {}^1/_6 k_2$$

Hence

$$k_1 = [3k_{MT}(H \rightarrow CH) - 3k_{MT}(CH_3 \rightarrow H)]$$

A more detailed discussion of these ideas together with a simplified method for extracting the individual elements of the Kubo–Sack matrix will be presented elsewhere.[28]

Registry No. *exo*-1 (R = Me), 75599-42-7; *endo*-1 (R = Me), 75576-71-5; *exo*-2 (R = Me), 68680-01-3; *endo*-2 (R = Me), 68586-68-5.

OM910569W

---

[61] Morris, G. A.; Freeman, R. *J. Magn. Reson.* **1979**, *29*, 433–462.

[62] Campbell, I. D.; Dobson, C. M.; Ratcliffe, R. G.; Williams, R. J. P. *J. Magn. Reson.* **1978**, *29*, 397–417.